Effect of $\mathcal{PT}$ symmetry in a parallel double-quantum-dot structure

Lian-Lian Zhang, Guo-Hui Zhan, Ze-Zhong Li, and Wei-Jiang Gong*

College of Sciences, Northeastern University, Shenyang 110819, China

(Received 2 November 2017; published 28 December 2017)

We present a comprehensive analysis about the effect of $\mathcal{PT}$-symmetric complex potentials on quantum transport through one parallel coupled double-quantum-dot structure. It is found that such potentials are able to eliminate the decoupling phenomenon while inducing the Fano effect, even under the situation of uniform dot-lead coupling. Moreover, the Fano line shape in the transmission function spectrum is opposite to that that arises from the detuning of the dot levels. We ascertain that this work can be helpful in understanding the quantum transport properties in the quantum systems with $\mathcal{PT}$ symmetry.

DOI: 10.1103/PhysRevA.96.062133

I. INTRODUCTION

$\mathcal{PT}$-symmetric systems, first proposed by Bender and his co-workers, are known as systems which do not obey parity ($\mathcal{P}$) and time-reversal ($\mathcal{T}$) symmetries separately, but exhibit a combined $\mathcal{PT}$ symmetry [1,2]. For such systems, the imaginary part of the complex potential V in the Hamiltonian is an antisymmetric function of the position $\mathbf{r}$, whereas its real part is a symmetric one, therefore $V(\mathbf{r}) = V^*(-\mathbf{r})$. As a result, the eigenvalue spectra have opportunities to remain real if the magnitude of the imaginary part of the potential does not exceed a threshold value. Since the $\mathcal{PT}$-symmetric systems show new properties that are not exhibited in the systems with a Hermitian Hamiltonian, they have attracted extensive interest during the past few years [3].

El-Ganainy *et al.* demonstrated that one coupled optical waveguide system with an engineered refractive index and gain or loss profile can be utilized to realize a $\mathcal{PT}$-symmetric structure [4]. Since then, numerous ideas and applications have been proposed for the $\mathcal{PT}$-symmetric systems in coupled optical wave guides [4–7], resonators [8–12], and optical lattices [13–16]. Various interesting phenomena have been observed, including fast evolution [17–20], power oscillation [21,22], unidirectional reflectionless [23], and coherent absorption [24–26]. Some researches have also been reported about $\mathcal{PT}$ symmetries in whispering gallery microcavities [27], and the mathematical structures of $\mathcal{PT}$ symmetries have been conceived [28]. Recently the $\mathcal{PT}$-symmetric optics has been realized experimentally on a chip at the 1550˜nm wavelength in two directly coupled high-Q silica-microtoroid resonators with balanced effective gain and loss [10]. In addition, Xiao *et al.* reported the experimental realization of passive $\mathcal{PT}$-symmetric quantum dynamics for single photons by temporally alternating photon losses in the quantum walk interferometers [29]. These works further warm up the exploration of the $\mathcal{PT}$-symmetric non-Hermitian systems.

Following the research progress of the $\mathcal{PT}$ symmetry, scientists began to think about its influence on the fundamental phenomena in the field of condensed matter physics, since the photons in coupled wave guides and optical lattices can be manipulated in a manner similar to the electrons in solids [30–32]. On the one hand, recent reports show that the optical analysis of solid-state systems has been extended to non-Hermitian systems [33–36]. For instance, $\mathcal{PT}$-symmetric non-Hermitian topological structures were theoretically investigated [37–40]. Evidence reveals that universal non-Hermiticity may alter topological regions [41], but topological properties are robust against local non-Hermiticity. Weimann and his partners found analytical closed-form solutions of topological $\mathcal{PT}$-symmetric interface states, and observe them through fluorescence microscopy in a passive $\mathcal{PT}$-symmetric dimerized photonic lattice [42]. On the other hand, some studies focused on the effects of the $\mathcal{PT}$ symmetry on the quantum transport behaviors in the quasi-one-dimensional systems, by taking finite $\mathcal{PT}$-symmetric potentials into account. It has been found that for one Fano-Anderson system, the $\mathcal{PT}$-symmetric potentials give rise to the changes from the perfect reflection to perfect transmission, as well as the behaviors for the absence or existence of the perfect reflection at one and two resonant frequencies [43]. In a non-Hermitian Aharonov-Bohm ring with one quantum dot (QD) embedded in each of its two arms, the asymmetric Fano profile will show up in the conductance spectrum just by non-Hermitian quantity in this system, by the presence of appropriate parameters [44]. Also in the rhombic QD ring with $\mathcal{PT}$ symmetry, the reciprocal reflection(transmission) and unidirectional transmission(reflection) appear in the axial (reflection) $\mathcal{PT}$-symmetric ring center [45]. Therefore, the $\mathcal{PT}$ symmetry indeed plays nontrivial roles in modulating the quantum transport process.

With respect to the influence of the $\mathcal{PT}$ symmetry on the quantum transport behavior, one should notice that it originates from the modification of the underlying quantum interference mechanism caused by the $\mathcal{PT}$ symmetry. Thus, it is necessary to clarify how the $\mathcal{PT}$ symmetry modifies the quantum interference. However, such a topic has not been discussed so far. In the present work, we would like to concentrate on one parallel coupled double-QD structure to observe its quantum transport behavior when the QD Hamiltonian becomes $\mathcal{PT}$-symmetric, by considering the $\mathcal{PT}$-symmetric complex potentials to act on QDs. Our standpoint is that the coupled-QD structure is one typical system that includes abundant basic physics and potential application [46]. Via calculation, it is found that in this process, the decoupling phenomenon can be eliminated, whereas the Fano effect comes into being, under the situation of uniform QD-lead coupling. Moreover,

*gwj@mail.neu.edu.cn

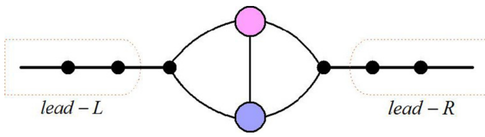

FIG. 1. Schematic of one non-Hermitian double-QD circuit. The QDs are influenced by $\mathcal{PT}$-symmetric complex on-site chemical potentials.

the Fano line shape in the transmission function spectrum is opposite to that arises from the detuning of the dot levels. We ascertain that this work can be helpful in understanding the quantum transport properties in the $\mathcal{PT}$-symmetric quantum systems.

II. THEORETICAL MODEL

The parallel-coupled double-QD structure that we consider is illustrated in Fig. 1. In such a system, two QDs couple to two semi-infinite one-dimensional leads in the parallel way, accompanied by the direct coupling between them. The Hamiltonian that describes the electronic motion in this system reads

$$H = H_C + H_D + H_T. \tag{1}$$

The first term is the Hamiltonian for the electrons in the two one-dimensional leads:

$$H_C = \sum_{j=-\infty}^{-1} t_0 c_j^\dagger c_{j-1} + \sum_{j=1}^{\infty} t_0 c_j^\dagger c_{j+1} + \text{H.c.}, \tag{2}$$

where $c_j^\dagger$ (c_j) is an operator to create (annihilate) an electron of the jth site in one lead, and t_0 is the intersite hopping energy. The second term describes the electron in the double QDs. It takes a form as

$$H_D = \sum_{l=1}^{2} \varepsilon_l d_l^\dagger d_l + (t_c d_1^\dagger d_2 + \text{H.c.}). \tag{3}$$

$d_l^\dagger$ (d_l) is the creation (annihilation) operator of electron in QD-l, and ε_l denotes the electron level in the corresponding QD. t_c describes the interdot coupling. Since we are interested in the influence of the $\mathcal{PT}$-symmetric complex potentials, the Coulomb interaction in the QDs has been ignored. The last term in the Hamiltonian denotes the electron tunneling between the leads and QDs. According to our assumption, it is given by

$$H_T = \sum_l (v_{Ll} d_l^\dagger c_{-1} + v_{Rl} d_l^\dagger c_1 + \text{H.c.}), \tag{4}$$

in which $v_{\alpha j}$ denotes the QD-lead coupling coefficient.

With the help of the transfer-matrix method, we can study the transport properties of this system, by deriving the analytical formula of the transmission coefficient. To begin, we would like to write out the wave function of the system as $|\psi\rangle = \sum_n c_n(t)|\phi_n\rangle + \sum_l d_l(t)|d_l\rangle$ with $|\phi_n\rangle = c_n^\dagger|0\rangle$ and $|d_l\rangle = d_l^\dagger|0\rangle$. By substituting expression of $|\psi\rangle$ into the Schrödinger equation $i\partial t|\psi\rangle = H|\psi\rangle$, the following coupled-mode equations can be obtained for the expansion coefficients c_n and d_l:

$$\begin{aligned} i\dot{c}_n &= t_0 c_{n-1}(1-\delta_{n,1}) + t_0 c_{n+1}(1-\delta_{n,-1}) \\ &\quad + \sum_l v_{Ll}^* d_l \delta_{n,-1} + \sum_l v_{Rl}^* d_l \delta_{n,1}, \end{aligned} \tag{5}$$

$$\begin{aligned} i\dot{d}_l &= \varepsilon_l d_l + t_c d_{l+1}\delta_{l,1} + t_c^* d_{l-1}\delta_{l,2} \\ &\quad + v_{Ll} c_{-1} + v_{Rl} c_1, \end{aligned} \tag{6}$$

where t_0 is assumed to be real. The stationary solution can be expressed in the following form:

$$c_n(t) = A_n e^{-i\omega t}, \qquad d_l(t) = B_l e^{-i\omega t}. \tag{7}$$

Then we can obtain the algebraic relationship of the amplitudes on each site; the following equations indicate that they are nested with each other:

$$\begin{aligned} \omega A_n &= t_0(1-\delta_{n,1})A_{n-1} + t_0(1-\delta_{n,-1})A_{n+1} \\ &\quad + \sum_l v_{Ll}^* B_l \delta_{n,-1} + \sum_l v_{Rl}^* B_l \delta_{n,1}, \end{aligned} \tag{8}$$

$$\begin{aligned} \omega B_l &= \varepsilon_l B_l + t_c B_{l+1}\delta_{l,1} + t_c^* B_{l-1}\delta_{l,2} \\ &\quad + v_{Ll} A_{-1} + v_{Rl} A_1. \end{aligned} \tag{9}$$

This allows us to deduce the equations that relate to A_{-1} and A_1:

$$\begin{aligned} (\omega - \tilde{\varepsilon}_{LL})A_{-1} &= t_0 A_{-2} + \tilde{\varepsilon}_{LR} A_1, \\ (\omega - \tilde{\varepsilon}_{RR})A_1 &= t_0 A_2 + \tilde{\varepsilon}_{RL} A_{-1}, \end{aligned} \tag{10}$$

with

$$\begin{aligned} \tilde{\varepsilon}_{\alpha\beta} &= \frac{1}{(\omega-\varepsilon_1)(\omega-\varepsilon_2) - |t_c|^2} \cdot \\ &\quad \times [(\omega-\varepsilon_1)v_{\alpha 2}^* v_{\beta 2} + t_c v_{\alpha 1}^* v_{\beta 2} \\ &\quad + t_c^* v_{\alpha 2}^* v_{\beta 1} + (\omega-\varepsilon_2) v_{\alpha 1}^* v_{\beta 1}]. \end{aligned}$$

Surely, $\tilde{\varepsilon}_{\alpha\alpha}$ and $\tilde{\varepsilon}_{\alpha\alpha'}$ can be viewed as the effective onsite energy and intersite hopping energy, respectively.

Next, the trial wave function should be introduced to describe the scattering properties in this system, given by

$$A_n = \begin{cases} e^{ikn} + re^{-ikn} & (n<0) \\ \tau e^{ikn} & (n>0) \end{cases}.$$

As a result, the matrix equation of r and τ can be written as

$$\begin{aligned} &\begin{bmatrix} (\omega-\tilde{\varepsilon}_{LL})e^{ik} - t_0 e^{2ik} & -\tilde{\varepsilon}_{LR}e^{ik} \\ -\tilde{\varepsilon}_{RL}e^{ik} & (\omega-\tilde{\varepsilon}_{RR})e^{ik} - t_0 e^{2ik} \end{bmatrix} \begin{bmatrix} r \\ \tau \end{bmatrix} \\ &= \begin{bmatrix} -(\omega-\tilde{\varepsilon}_{LL})e^{-ik} + t_0 e^{-2ik} \\ \tilde{\varepsilon}_{RL}e^{-ik} \end{bmatrix}. \end{aligned} \tag{11}$$

Therefore, the analytical form of the transmission amplitude τ can be figured out:

$$\tau = \frac{t_0\tilde{\varepsilon}_{RL}(e^{ik} - e^{-ik})}{(t_0 e^{-ik} - \tilde{\varepsilon}_{LL})(t_0 e^{-ik} - \tilde{\varepsilon}_{RR}) - \tilde{\varepsilon}_{LR}\tilde{\varepsilon}_{RL}}. \tag{12}$$

With the help of this formula, we are able to investigate the transmission function property by using the relation of $T(\omega) = |\tau|^2$.

In our considered geometry, the effect of the $\mathcal{P}$ operator is to let $\mathcal{P}d_1\mathcal{P} = d_2$ with the linear chain as the mirror axis, and the effect of the $\mathcal{T}$ operator is $\mathcal{T}i\mathcal{T} = -i$. Thus, it is not difficult to find that the Hamiltonian is invariant under the combined operation $\mathcal{PT}$, under the condition of $\varepsilon_1 = \varepsilon_2^*$ for the case of uniform QD-lead coupling. Moreover, since the QDs couple to the two metallic leads simultaneously, one quantum ring is built. Therefore, $v_{\alpha l}$ will become complex when local magnetic flux is introduced. Under the gauge transformation, these phase factors can be allocated differently. It is known that for one Hermitian Hamiltonian, the physical variables will not be influenced by these differences. We would like to emphasize that this physical picture also applies to the non-Hermitian system. In this work, we choose the symmetric gauge with the phase factor distributed averagely to the four tunneling amplitudes, i.e., $v_{L1} = v_0 e^{i\phi/4}$, $v_{L2} = v_0 e^{-i\phi/4}$, $v_{R1} = v_0 e^{-i\phi/4}$, and $v_{R2} = v_0 e^{i\phi/4}$, where $\phi = 2\pi\frac{\Phi}{\phi_0}$ is the magnetic flux phase factor with Φ being the magnetic flux and $\phi_0 = \frac{h}{e}$.

In this work, we would like to introduce the $\mathcal{PT}$-symmetric complex potentials to the two QDs to present the influences of $\mathcal{PT}$ symmetry on the quantum transport through the parallel-coupled double-QD structure. To do so, we suppose $\varepsilon_1 = \varepsilon - i\gamma$ and $\varepsilon_1 = \varepsilon + i\gamma$, respectively, to perform discussion. In experiment, the $\mathcal{PT}$-symmetric complex potentials can be realized by considering the energy gain and loss [47]. In such a case, $\tilde{\varepsilon}_{\alpha\beta}$ can be rewritten as

$$\tilde{\varepsilon}_{LL(RR)} = \frac{2v_0^2\left(\omega - \varepsilon + t_c \cos\frac{\phi}{2}\right)}{(\omega-\varepsilon)^2 + \gamma^2 - t_c^2},$$
$$\tilde{\varepsilon}_{LR(RL)} = \frac{2v_0^2\left[(\omega-\varepsilon)\cos\frac{\phi}{2} \pm \gamma\sin\frac{\phi}{2} + t_c\right]}{(\omega-\varepsilon)^2 + \gamma^2 - t_c^2}. \quad (13)$$

III. NUMERICAL RESULTS AND DISCUSSIONS

With the theory developed in Sec. II, we continue to discuss the transmission function spectrum of one parallel double-QD structure, by considering the presence of $\mathcal{PT}$-symmetric complex potentials. In the context, we take the parameter values as $t_0 = 1.0$, $\varepsilon = 0$, and $t_c = v_0 = 0.5$ to perform our numerical calculation.

First, we ignore the presence of $\mathcal{PT}$-symmetric complex potentials to investigate the transmission function properties. One can clearly find that in such a case, $\tilde{\varepsilon}_{\alpha\beta} = \frac{2v_0^2}{\omega-\varepsilon-t_c}$ in the absence of magnetic flux, whereas in the case of $\phi = 2\pi$, there will be $\tilde{\varepsilon}_{\alpha\alpha} = -\tilde{\varepsilon}_{\alpha\alpha'} = \frac{2v_0^2}{\omega-\varepsilon+t_c}$. Thus, one can get the result that

$$T(\omega)|_{\phi=0(2\pi)} = |\tau|^2 = \frac{4\Gamma_0^2}{\left(\frac{t_0^2-2v_0^2}{t_0^2}\omega - \varepsilon \mp t_c\right)^2 + 4\Gamma_0^2}. \quad (14)$$

In this formula, $\Gamma_0 = 4v_0^2\sqrt{1-(\omega/2t_0)^2}/t_0$, which can be considered to be the coupling strength between the QDs and leads. Under the situation of $v_0 = \frac{1}{2}t_0$, its profiles show up as peaks at the points $\omega = 2(\varepsilon \pm t_c)$, respectively, in the above two cases. Such a result can be clearly observed in Figs. 2(a)–2(b). In fact, this is exactly caused by the occurrence of the decoupling mechanism. It can be analyzed as follows. For the double-QD molecule, the molecular levels are $E_\mp = \varepsilon \mp t_c$, respectively, and the unitary matrix related to the "atomic" and "molecular" states takes a form as $[\boldsymbol{\eta}] = \frac{1}{\sqrt{2}}\begin{bmatrix}-1 & 1\\ 1 & 1\end{bmatrix}$. One can then know that the coupling between the bonding state and lead-α, i.e., $w_{-\alpha}$, proportional to $([\boldsymbol{\eta}]_{11}^\dagger + e^{i\phi/2}[\boldsymbol{\eta}]_{21}^\dagger)$, is exactly equal to zero, so the bonding state decouples from the leads completely in the absence of magnetic flux. Instead, for the coupling between the antibonding state and lead-α, it is expressed as $w_{+\alpha} = v_0([\boldsymbol{\eta}]_{12}^\dagger + e^{i\phi/2}[\boldsymbol{\eta}]_{22}^\dagger)$. As a consequence, for the case of $\phi = 0$ (2π), it is the nonzero $w_{+\alpha}$ ($w_{-\alpha}$) that leads to the peak of the transmission function spectrum.

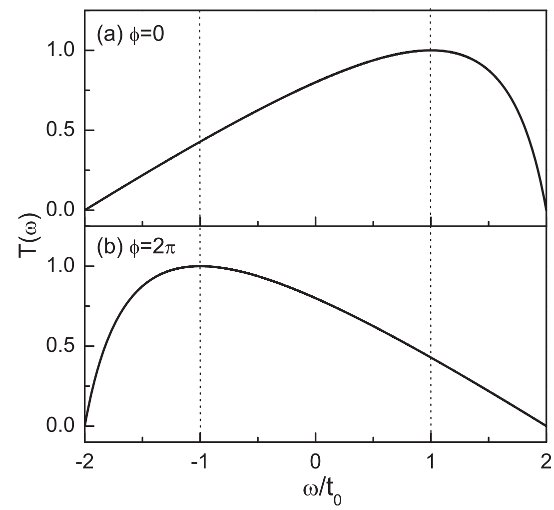

FIG. 2. (a, b) Transmission function spectra in the absence of $\mathcal{PT}$-symmetric complex potentials, in the cases of $\phi = 0$ and 2π, respectively.

Next, we take $\varepsilon_1 = \varepsilon - i\gamma$ and $\varepsilon_2 = \varepsilon + i\gamma$ to evaluate the influence of the $\mathcal{PT}$-symmetric complex potentials on the quantum transport in this system. Accordingly, there will be $\tilde{\varepsilon}_{\alpha\beta} = \frac{2v_0^2(\omega-\varepsilon+t_c)}{(\omega-\varepsilon)^2+\gamma^2-t_c^2}$ in the case of $\phi = 0$, and if $\phi = 2\pi$, $\tilde{\varepsilon}_{\alpha\alpha} = -\tilde{\varepsilon}_{\alpha\alpha'} = \frac{2v_0^2(\omega-\varepsilon-t_c)}{(\omega-\varepsilon)^2+\gamma^2-t_c^2}$. In such cases, we would like to express the transmission amplitude as

$$\tau = \frac{2i\tilde{\varepsilon}_{\alpha\alpha}\sin k}{2\tilde{\varepsilon}_{\alpha\alpha}e^{ik} - t_0}. \quad (15)$$

It is easy to find that $\tilde{\varepsilon}_{\alpha\alpha}$ is a key quantity to govern the transmission amplitude of this system. To be specific, in the cases of $\phi = 0(2\pi)$, $\tilde{\varepsilon}_{\alpha\alpha}$ will encounter its zero value at the positions of $\omega = \varepsilon \mp t_c$, respectively. This exactly leads to the fact that the transmission amplitude τ is equal to zero. Thus, the decoupling phenomena transform into antiresonances, in the presence of $\mathcal{PT}$-symmetric complex potentials. Therefore, one can conclude that the $\mathcal{PT}$-symmetric complex potentials play a significant role in modifying the quantum transport in this system. In Fig. 3 we present the numerical results of the transmission function by choosing $\gamma = 0.1$, 0.3, and 0.5. In Figs. 3(a)–3(b), it clearly shows that the increase of γ only widens the antiresonance valley but cannot change the antiresonance position. On the other hand, we can find that in the case of $\phi \neq 2m\pi$ ($m \in$ integers), $\tilde{\varepsilon}_{\alpha\alpha'}$ will have no opportunity to be equal to zero. And, then, no antiresonance will occur in the quantum transport process. For instance, when local magnetic flux is introduced with $\phi = \pi$, $\tilde{\varepsilon}_{\alpha\alpha} = \frac{2v_0^2(\omega-\varepsilon)}{(\omega-\varepsilon)^2+\gamma^2-t_c^2}$ and $\tilde{\varepsilon}_{RL} = \frac{2v_0^2(t_c-\gamma)}{(\omega-\varepsilon)^2+\gamma^2-t_c^2}$. Surely, if $\gamma = t_c$, there will be $\tilde{\varepsilon}_{RL} \equiv 0$, which exactly eliminates the quantum transport process in the whole energy region [see Fig. 3(c)].

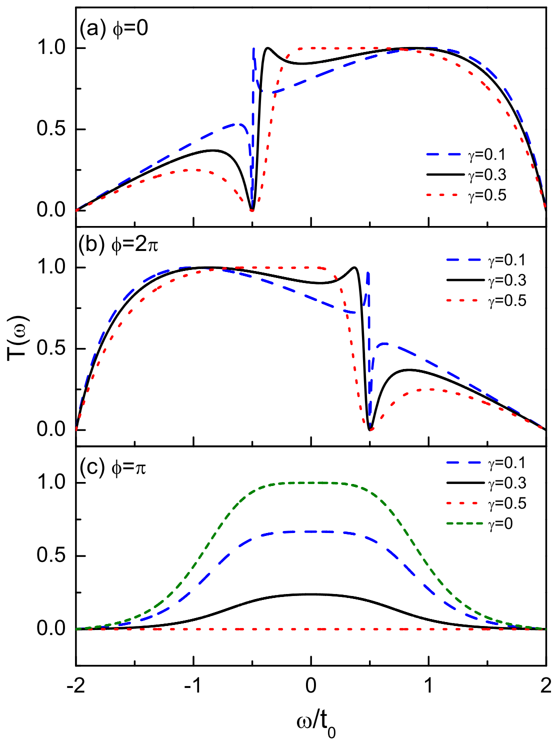

FIG. 3. Spectra of transmission function $T(\omega)$ in the presence of $\mathcal{PT}$-symmetric complex potentials. The values of γ are taken to be 0.1, 0.3, and 0.5, respectively. (a–c) The magnetic flux phase factor ϕ is equal to 0, 2π, and π, respectively.

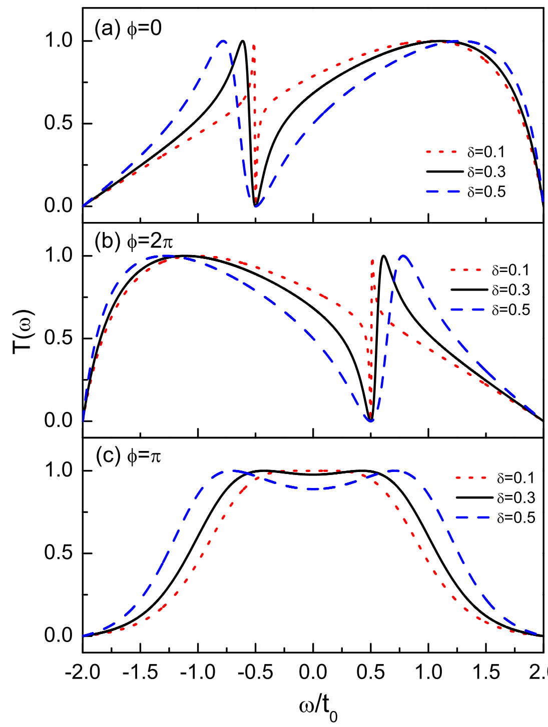

FIG. 4. Spectra of $T(\omega)$ vs ω due to the detuning of QD levels, with $\varepsilon_1 = \varepsilon + \delta$ and $\varepsilon_2 = \varepsilon - \delta$. The values of $\delta = 0.1$, 0.3, and 0.5, respectively. (a–c) Transmission function spectra in the cases of $\phi = 0$, 2π, and π, respectively.

In Figs. 3(a)–3(b), we can readily find that around the antiresonance point, the transmission function profile shows up as the Fano line shape. This exactly means that the Fano effect takes place, when the $\mathcal{PT}$-symmetric complex potentials act on the QDs. It is necessary for us to clarify the underlying physics of the Fano effect in such a case. For this reason, we would like to detune the QD levels by considering $\varepsilon_1 = \varepsilon + \delta$ and $\varepsilon_2 = \varepsilon - \delta$ (δ is real), to compare the change of the transmission function spectrum. This can also be viewed as the breaking of the inversion symmetry of the double QDs. It can be found that in such a case, the expression of the transmission amplitude is the same as the result in Eq. (15), except the change of the denominator of $\tilde{\varepsilon}_{\alpha\beta}$ to be $(\omega - \varepsilon)^2 - \delta^2 - t_c^2$. Thus, the antiresonance also occurs at the point of $\omega = \varepsilon \mp t_c$, in the case of $\phi = 0(2\pi)$. Then we plot the transmission function spectra in Fig. 4. One can observe that in the case of $\phi = 0(2\pi)$, the transmission function spectra also exhibit the Fano line shapes around the antiresonance points. However, in such a case, the asymmetry manner of the Fano line shapes are different from those induced by the $\mathcal{PT}$-symmetric complex potentials. In other words, when the $\mathcal{PT}$-symmetric complex potentials change to be the detuning of the QD levels, the Fano line shape in the transmission function spectrum will be reversed. We can then understand the special influence of the $\mathcal{PT}$-symmetric complex potentials on the quantum transport in the parallel coupled double-QD structure. In addition, it shows in Fig. 4(c) that in the case of $\phi = \pi$, the magnitude of the transmission function cannot be suppressed but the spectrum width is increased, when the detuning of the QD levels is enhanced.

In the following, we would like to present a detailed analysis about the Fano effect in the above two cases. As is known, the Fano effect is usually discussed by transforming the expression of $T(\omega)$ into its Fano form, and the parameters in the Fano form are helpful for understanding the Fano effect [48]. Following this idea, we next take the case of $\phi = 0$ as an example to perform discussion. After a straightforward deduction, in the above two cases, both the Fano forms of the transmission function can be written as

$$T(\omega) = \frac{|e + q|^2}{e^2 + 1}, \tag{16}$$

in which the relevant parameters are given by $q = 0$ and $e = \frac{2\tilde{\varepsilon}_{\alpha\alpha} \sin k}{2\tilde{\varepsilon}_{\alpha\alpha} \cos k - t_0}$. By using the relation $\omega = 2t_0 \cos k$, the parameter e can be reexpressed as

$$e = \frac{\Gamma_0(\omega - \varepsilon + t_c)}{\Gamma_0(\omega - \varepsilon + t_c) - 2\left[(\omega - \varepsilon)^2 + \gamma^2 - t_c^2\right]} \tag{17}$$

in the case of finite $\mathcal{PT}$-symmetric potentials. On the other hand, when the QD levels are detuned, it is given by

$$e = \frac{\Gamma_0(\omega - \varepsilon + t_c)}{\Gamma_0(\omega - \varepsilon + t_c) - 2\left[(\omega - \varepsilon)^2 - \delta^2 - t_c^2\right]}. \tag{18}$$

In Fig. 5 we plot the curves of e in these two cases. One can find that around the antiresonance point, the variation manner of e determines the Fano line shape of the transmssion function spectrum. Such a result is easy to understand by approximating the expression of e. Near the antiresonance point, the expression of parameter e can be simplified as $e \approx -\frac{\Gamma_0}{2\gamma^2}(\omega - \varepsilon + t_c)$ and $e \approx \frac{\Gamma_0}{2\delta^2}(\omega - \varepsilon + t_c)$, respectively.

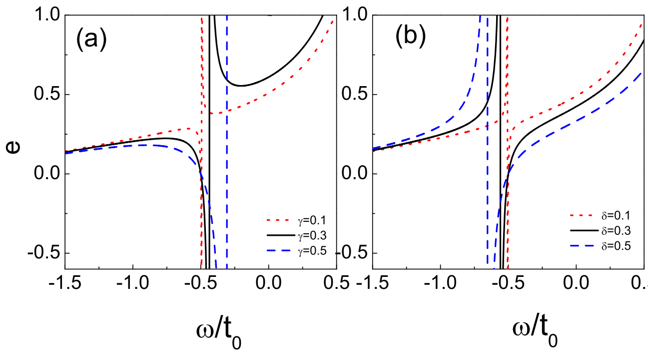

FIG. 5. Spectra of e in the Fano form of the transmission function. (a) Influence of the $\mathcal{PT}$-symmetric complex potentials, in the cases of $\gamma = 0.1$, 0.3, and 0.5, respectively. (a–c) Results of detuning the QD levels with $\delta = 0.1$, 0.3, and 0.5, respectively.

Such a difference exactly gives rise to the appearance of the opposite Fano line shapes.

One can be sure that the Fano effect arises from destructive quantum interference between the nonresonant and resonant channels. Thus, in order to reveal the special property of the Fano interference, the two kinds of channels should be presented. For our considered system, the role of $\mathcal{PT}$-symmetric potentials in driving the Fano effect can also be further understood from its contribution to the nonresonant and resonant channels. Then in the following we try to transform the double QDs into the molecular-orbit representation to analyze the properties of the nonresonant and resonant channels involved.

We first discuss the case of detuning the QD levels, since its physics picture is relatively clear. In such a case, the eigenlevels of the double-QD molecule are easy to figure out, i.e., $E_- = \varepsilon - t_c \csc\vartheta$ and $E_+ = \varepsilon + t_c \csc\vartheta$, respectively, where $\vartheta = \arctan\frac{t_c}{\delta}$. The corresponding molecular states are $\Psi_- = \frac{1}{\sqrt{2}}[-\sin\frac{\vartheta}{2}, \cos\frac{\vartheta}{2}]^T$ and $\Psi_+ = \frac{1}{\sqrt{2}}[\cos\frac{\vartheta}{2}, \sin\frac{\vartheta}{2}]^T$, respectively. Therefore, the unitary matrix $[\boldsymbol{\eta}]$ can be given by

$$[\boldsymbol{\eta}] = \frac{1}{\sqrt{2}}\begin{bmatrix} -\sin\frac{\vartheta}{2} & \cos\frac{\vartheta}{2} \\ \cos\frac{\vartheta}{2} & \sin\frac{\vartheta}{2} \end{bmatrix}. \tag{19}$$

This allows us to get the coupling coefficients between the molecular states and the leads: $w_{-\alpha} = (\cos\frac{\vartheta}{2} - \sin\frac{\vartheta}{2})v_0$ and $w_{+\alpha} = (\cos\frac{\vartheta}{2} + \sin\frac{\vartheta}{2})v_0$. Accordingly, the coupling strengths between the molecular states and lead-α are $\Gamma_-^\alpha = (1 - \sin\vartheta)\Gamma_0$ and $\Gamma_+^\alpha = (1 + \sin\vartheta)\Gamma_0$, respectively. For a small δ, there will be $\Gamma_-^\alpha \ll \Gamma_+^\alpha$, hence the resonant and nonresonant channels for the Fano effect are constructed. To be concrete, the coupling between the bonding state provides the resonant channel of the Fano interference, while the antibonding state contributes to the nonresonant channel. After this discussion, the properties of the two channels can be clarified. Some previous works have described the quantum interference mechanism between the two channels by using the Feynman-path language [49]. This can also be helpful for further understanding the Fano effect.

Following the above analysis, we turn to the discussion about the nonresonant and resonant channels constructed by the $\mathcal{PT}$-symmetric potentials. Note that since the QD Hamiltonian is non-Hermitian, the representation transformation will exhibit its new form. Surely in such a case, the eigenlevels of the double-QD molecule can be written out by diagonalizing the QD Hamiltonian, i.e., $E_- = \varepsilon - t_c\cos\theta$ and $E_+ = \varepsilon + t_c\cos\theta$, respectively, with $\theta = \arcsin\frac{\gamma}{t_c}$ (under the condition of $\gamma \leqslant t_c$). However, considering the $\boldsymbol{\eta}$ matrix is not unitary, we can write out the corresponding molecular states in the forms as $\Psi_- = \frac{1}{\sqrt{2\cos\theta}}[-e^{i\theta},1]^T$ and $\Psi_+ = \frac{1}{\sqrt{2\cos\theta}}[e^{-i\theta},1]^T$, which obey an alternative orthonormal relation: $\Psi_+^\dagger\sigma_x\Psi_+ = 1$, $\Psi_+^\dagger\sigma_x\Psi_- = 0$, and $\Psi_-^\dagger\sigma_x\Psi_- = -1$, with σ_x being the Pauli matrix [50]. Then the $\boldsymbol{\eta}$ matrix transforms into

$$[\boldsymbol{\eta}] = \frac{1}{\sqrt{2\cos\theta}}\begin{bmatrix} -e^{i\theta} & e^{-i\theta} \\ 1 & 1 \end{bmatrix}. \tag{20}$$

Accordingly, the coupling coefficients between the molecular states and the leads change to be $w_{-\alpha} = \frac{(1-e^{-i\theta})v_0}{\sqrt{2\cos\theta}}$ and $w_{+\alpha} = \frac{(1+e^{i\theta})v_0}{\sqrt{2\cos\theta}}$, and the coupling strengths between the molecular states and lead-α are given as $\Gamma_-^\alpha = \frac{\cos\theta-1}{\cos\theta}\Gamma_0$ and $\Gamma_+^\alpha = \frac{\cos\theta+1}{\cos\theta}\Gamma_0$. One can clearly find that for a nonzero γ, there will be $\Gamma_-^\alpha < 0$. This exactly reflects the fundamental difference between the influences of the $\mathcal{PT}$-symmetric potentials and the detuning of the QD levels. Surely, in the case of $\gamma \ll t_c$, the condition of $|\Gamma_-^\alpha| \ll \Gamma_+^\alpha$ can also be satisfied, so the resonant and nonresonant channels are able to be achieved for the Fano interference. It should also be noticed that due to $\Gamma_- < 0$, the phase of the electron wave will be different from that in the case of nonzero δ. This inevitably leads to an alternative Fano interference mode. Up to now, one can find that in such two cases, the eigenlevels and the coupling manner between the molecular states and the leads change in different ways. This certainly leads to the different Fano interference modes. After the discussion above, we can further understand the effect of the $\mathcal{PT}$-symmetric complex potentials on the quantum transport through the parallel double-QD system.

IV. SUMMARY

To summarize, by taking one parallel coupled double-QD system, we have presented a comprehensive analysis of the effect of $\mathcal{PT}$-symmetric complex potentials on quantum transport through one non-Hermitian system. As a result, it has been found that such potentials take pronounced effects to the transport properties of the parallel-coupled QD system, manifested as the occurrence of Fano antiresonance. However, such a kind of Fano effect is completely different from that induced by the detuning of the QD levels. Next, we have analyzed the two kinds of Fano effects via reexpressing the transmission function formula into its Fano form and transforming such a system into its molecular-orbit representation. Then the underlying physics of the Fano effect has been clarified. We believe that this work can be helpful in further understanding the special change of quantum transport behaviors modified by the $\mathcal{PT}$-symmetric complex potentials.

ACKNOWLEDGMENT

W.-J.G. thanks Qi Zhang for his helpful discussions.

[1] C. M. Bender and S. Boettcher, Phys. Rev. Lett. **80**, 5243 (1998).
[2] C. M. Bender, D. C. Brody, and H. F. Jones, Phys. Rev. Lett. **89**, 270401 (2002).
[3] V. V. Konotop, J. Yang, and D. A. Zezyulin, Rev. Mod. Phys. **88**, 035002 (2016).
[4] R. El-Ganainy, K. G. Makris, D. N. Christodoulides, and Z. H. Musslimani, Opt. Lett. **32**, 2632 (2007).
[5] A. Ruschhaupt, F. Delgado, and J. G. Muga, J. Phys. A: Math. Gen. **38**, L171 (2005).
[6] Z. H. Musslimani, K. G. Makris, R. El-Ganainy, and D. N. Christodoulides, Phys. Rev. Lett. **100**, 030402 (2008).
[7] A. Guo, G. J. Salamo, D. Duchesne, R. Morandotti, M. Volatier-Ravat, V. Aimez, G. A. Siviloglou, and D. N. Christodoulides, Phys. Rev. Lett. **103**, 093902 (2009).
[8] H. Jing, S. K. Özdemir, X. Y. Lü, J. Zhang, L. Yang, and F. Nori, Phys. Rev. Lett. **113**, 053604 (2014); H. Jing, S. K. Özdemir, Z. Geng, J. Zhang, X. Y. Lu, B. Peng, L. Yang, and F. Nori, Sci. Rep. **5**, 9663 (2015).
[9] B. Peng, S. K. Özdemir, F. Lei, F. Monifi, M. Gianfreda, G. L. Long, S. Fan, F. Nori, C. M. Bender, and L. Yang, Nat. Phys. **10**, 394 (2014); B. Peng, S. K. Özdemir, S. Rotter, H. Yilmaz, M. Liertzer, F. Monifi, C. M. Bender, F. Nori, and L. Yang, Science **346**, 328 (2014).
[10] L. Chang, X. Jiang, S. Hua, C. Yang, J. Wen, L. Jiang, G. Li, G. Wang, and M. Xiao, Nat. Photon. **8**, 524 (2014).
[11] X. Y. Lü, H. Jing, J. Y. Ma, and Y. Wu, Phys. Rev. Lett. **114**, 253601 (2015).
[12] Z. P. Liu, J. Zhang, S. K. Özdemir, B. Peng, H. Jing, X. Y. Lü, C. W. Li, L. Yang, F. Nori, and Y. X. Liu, Phys. Rev. Lett. **117**, 110802 (2016).
[13] C. Hang, G. Huang, and V. V. Konotop, Phys. Rev. Lett. **110**, 083604 (2013).
[14] Z. Zhang, Y. Zhang, J. Sheng, L. Yang, M. A. Miri, D. N. Christodoulides, B. He, Y. Zhang, and M. Xiao, Phys. Rev. Lett. **117**, 123601 (2016).
[15] A. Regensburger, C. Bersch, M. A. Miri, G. Onishchukov, D. N. Christodoulides, and U. Peschel, Nature (London) **488**, 167 (2012).
[16] M. Wimmer, A. Regensburger, M. A. Miri, C. Bersch, D. N. Christodoulides, and U. Peschel, Nat. Commun. **6**, 7782 (2015).
[17] C. M. Bender, D. C. Brody, H. F. Jones, and B. K. Meister, Phys. Rev. Lett. **98**, 040403 (2007).
[18] A. Mostafazadeh, Phys. Rev. Lett. **99**, 130502 (2007).
[19] U. Günther and B. F. Samsonov, Phys. Rev. Lett. **101**, 230404 (2008).
[20] C. Zheng, L. Hao, and G. L. Long, Philos. Trans. R. Soc. A **371**, 20120053 (2013).
[21] C. E. Rüter, K. G. Makris, R. El-Ganainy, D. N. Christodoulides, M. Segev, and D. Kip, Nat. Phys. **6**, 192 (2010).
[22] M. Chitsazi, H. Li, F. M. Ellis, and T. Kottos, Phys. Rev. Lett. **119**, 093901 (2017).
[23] L. Feng, Y. L. Xu, W. S. Fegadolli, M.-H. Lu, J. E. B. Oliveira, V. R. Almeida, Y. F. Chen, and A. Scherer, Nat. Mater. **12**, 108 (2013).
[24] Y. D. Chong, L. Ge, H. Cao, and A. D. Stone, Phys. Rev. Lett. **105**, 053901 (2010).
[25] W. Wan, Y. Chong, L. Ge, H. Noh, A. D. Stone, and H. Cao, Science **331**, 889 (2011).
[26] Y. Sun, W. Tan, H. Q. Li, J. Li, and H. Chen, Phys. Rev. Lett. **112**, 143903 (2014).
[27] Z. H. Zhou, F. J. Shu, Z. Shen, C. H. Dong, and G. C. Guo, Sci. China-Phys. Mech. Astron. **58**, 114208 (2015).
[28] A. Uhlmann, Sci. China-Phys. Mech. Astron. **59**, 630301 (2016).
[29] L. Xiao, X. Zhan, Z. H. Bian, K. K. Wang, X. Zhang, X. P. Wang, J. Li, K. Mochizuki, D. Kim, N. Kawakami, W. Yi, H. Obuse, B. C. Sanders, and P. Xue, Nat. Phys. **13**, 1117 (2017).
[30] A. B. Khanikaev, S. H. Mousavi, W. K. Tse, M. Kargarian, A. H. MacDonald, and G. Shvets, Nat. Mater. **12**, 233 (2013).
[31] M. C. Rechtsman, J. M. Zeuner, Y. Plotnik, Y. Lumer, D. Podolsky, F. Dreisow, S. Nolte, M. Segev, and A. Szameit, Nature (London) **496**, 196 (2013).
[32] L. Lu, J. D. Joannopoulos, and M. Soljačič, Nat. Photon. **8**, 821 (2014).
[33] G. Q. Liang and Y. D. Chong, Phys. Rev. Lett. **110**, 203904 (2013).
[34] J. M. Zeuner, M. C. Rechtsman, Y. Plotnik, Y. Lumer, S. Nolte, M. S. Rudner, M. Segev, and A. Szameit, Phys. Rev. Lett. **115**, 040402 (2015).
[35] S. Malzard, C. Poli, and H. Schomerus, Phys. Rev. Lett. **115**, 200402 (2015).
[36] C. Poli, M. Bellec, U. Kuhl, F. Mortessagne, and H. Schomerus, Nat. Commun. **6**, 6710 (2015).
[37] C. Yuce, Phys. Lett. A **378**, 2024 (2014).
[38] A. K. Harter, T. E. Lee, and Y. N. Joglekar, Phys. Rev. A **93**, 062101 (2016).
[39] X. Wang, T. Liu, Y. Xiong, and P. Tong, Phys. Rev. A **92**, 012116 (2015).
[40] M. Klett, H. Cartarius, D. Dast, J. Main, and G. Wunner, Phys. Rev. A **95**, 053626 (2017).
[41] Y. C. Hu and T. L. Hughes, Phys. Rev. B **84**, 153101 (2011).
[42] S. Weimann, M. Kremer, Y. Plotnik, Y. Lumer, S. Nolte, K. G. Makris, M. Segev, M. C. Rechtsman, and A. Szameit, Nat. Mater. **16**, 433 (2017).
[43] B. Zhu, R. Lü, and S. Chen, Phys. Rev. A **91**, 042131 (2015).
[44] Q. B. Zeng, S. Chen, and R. Lü, arXiv:1608.00065v2.
[45] L. Jin, X. Z. Zhang, G. Zhang, and Z. Song, Sci. Rep. **6**, 20976 (2016).
[46] J. C. Chen, A. M. Chang, and M. R. Melloch, Phys. Rev. Lett. **92**, 176801 (2004).
[47] N. X. A. Rivolta, H. Benisty, and B. Maes, Phys. Rev. A **96**, 023864 (2017).
[48] A. E. Miroshnichenko, S. FlachYuri, and S. Kivshar, Rev. Mod. Phys. **82**, 2257 (2010).
[49] W. Gong, Y. Zheng, Y. Liu, and T. Lü, Physica E **40**, 618 (2008).
[50] L. R. Mead and D. Garfinkle, AIP Advances **7**, 085001 (2017).